Journal of Affective Disorders 318 (2022) 246–254

Contents lists available at ScienceDirect

Journal of Affective Disorders

journal homepage: www.elsevier.com/locate/jad

Research paper

Diagnosis of late-life depression using structural equation modeling and dynamic effective connectivity during resting fMRI

Raquel Cosío-Guirado [a,*], Carles Soriano-Mas [a,b,c,**], Inés del Cerro [b], Mikel Urretavizcaya [b,c,d], José M. Menchón [b,c,d], Virginia Soria [b,c,d], Cristina Cañete-Massé [a,e], Maribel Peró-Cebollero [a,e,f], Joan Guàrdia-Olmos [a,e,f]

[a] Department of Social Psychology and Quantitative Psychology, Universitat de Barcelona, Barcelona, Spain
[b] Bellvitge Biomedical Research Institute-IDIBELL, Department of Psychiatry, Bellvitge University Hospital, Barcelona, Spain
[c] Network Center for Biomedical Research on Mental Health (CIBERSAM), Carlos III Health Institute (ISCIII), Madrid, Spain
[d] Department of Clinical Sciences, Bellvitge Campus, Universitat de Barcelona-UB, Barcelona, Spain
[e] UB Institute of Complex Systems, Universitat de Barcelona, Spain
[f] Institute of Neuroscience, Universitat de Barcelona, Spain

ARTICLE INFO

Keywords:
Dynamic effective connectivity
Structural equation modeling
fMRI
Late-life depression
Major depressive disorder
Default mode network

ABSTRACT

Background: Late-life depression (LLD) is characterized by cognitive and social impairments. Determining neurobiological alterations in connectivity in LLD by means of fMRI may lead to a better understanding of the neural basis underlying this disorder and more precise diagnostic markers. The primary objective of this paper is to identify a structural model that best explains the dynamic effective connectivity (EC) of the default mode network (DMN) in LLD patients compared to controls.

Methods: Twenty-seven patients and 29 healthy controls underwent resting-state fMRI during a period of eight minutes. In both groups, jackknife correlation matrices were generated with six ROIs of the DMN that constitute the posterior DMN (pDMN). The different correlation matrices were used as input to estimate each structural equation model (SEM) for each subject in both groups incorporating dynamic effects.

Results: The results show that the proposed LLD diagnosis algorithm achieves perfect accuracy in classifying LLD patients and controls. This differentiation is based on three aspects: the importance of ROIs 4 and 6, which seem to be the most distinctive among the subnetworks; the shape that the specific connections adopt in their networks, or in other words, the directed connections that are established among the ROIs in the pDMN for each group; and the number of dynamic effects that seem to be greater throughout the six ROIs studied [$t = 54.346$; $df = 54$; $p < .001$; *95 % CI difference* = 5.486–5.906].

Limitations: The sample size was moderate, and the participants continued their current medications.

Conclusions: The network models that we developed describe a pattern of dynamic activation in the pDMN that may be considered a possible biomarker for LLD, which may allow early diagnosis of this disorder.

1. Introduction

The study of brain connectivity in major depressive disorder (MDD) has noticeably attracted considerable interest in recent years. This serious mental disorder is characterized by a sustained negative affect along with difficulties in experiencing a positive affect, deficits in affect regulation and cognitive control, anhedonia, and the presence of cognitive biases (American Psychiatric Association, 2013; Joormann and Stanton, 2016). According to recent estimations, in the general community, up to 7 % of adults older than 60 years of age are affected by MDD, which in this group is known as the late-life depression (LLD) (Wen et al., 2022). LLD is particularly susceptible to poor outcomes, including no remission, aggravation of comorbidities, and diminished daily functioning (Gunning et al., 2021), as well as increasing the risk of

* Correspondence to: R.C. Guirado, Facultat de Psicología, Universitat de Barcelona, Passeig de la Vall d'Hebrón, 171, 08035 Barcelona, Spain.
** Correspondence to: C. Soriano-Mas, Bellvitge Biomedical Research Institute-IDIBELL, Dep. of Psychiatry, Bellvitge University Hospital, Feixa Llarga, s/n, 08907 L'Hospitalet de Llobregat, Spain.
E-mail addresses: raquelcg18@gmail.com (R. Cosío-Guirado), csoriano@idibell.cat (C. Soriano-Mas).

https://doi.org/10.1016/j.jad.2022.09.010
Received 28 July 2022; Received in revised form 2 September 2022; Accepted 6 September 2022
Available online 10 September 2022

dementia and mortality (Manning et al., 2019). Hence, LLD results in significant costs for individuals and society as a whole since it is a leading contributor to disability worldwide (Sartorius, 2001; Wen et al., 2022). However, its neuropathological mechanisms remain unclear.

The perspective of effective connectivity (EC) for the study of brain connectivity furnishes deep insights into brain dynamics and neuronal interactions (Friston, 2011; Zarghami and Friston, 2020). EC reveals the influence that a neuronal system exerts over another and vice versa and the direction of such effects (Friston, 2011; Friston et al., 2014; Zarghami and Friston, 2020). EC analyses engender a variety of causal models of distributed brain connections, and the network best suiting the data is selected (Friston, 2011; Razi et al., 2015; Razi and Friston, 2016; Zarghami and Friston, 2020). Structural equation modeling (SEM) is among the most prevalent methods for EC analysis, allowing an analysis of causal influences by examining the support that a given neural model accumulates given the covariance observed in the data (Inman et al., 2012). The combination of SEM and functional magnetic resonance imaging (fMRI) serves as a powerful tool for time series network analysis and estimates of intrinsic EC (Razi et al., 2017). For such analyses, brain connectivity should be conceived in terms of dynamic activity, which may be conceived in terms of connectivity estimates across temporal lags (lag 1 in this study) (Friston, 2011; Zarghami and Friston, 2020). Accordingly, we can estimate the effect that an ROI at a moment t exerts over another ROI at a previous time, $t + 1$, that is, how the activity occurring at a certain region of the network influences later signals at a different location (Beltz and Gates, 2017; Gates et al., 2011; Zhang et al., 2020).

However, the assessment of dynamic EC in MDD remains minimally explored, most specifically using the SEM approach. However, two recent studies show the suitability of this approach to assess dynamic EC. First, the research by Zhang et al. (2020) is an example of the implementation of group iterative multiple model estimation (GIMME) to estimate dynamic EC in the field of neurolinguistics. Second, Figueroa-Jiménez et al. (2021) appraised dynamic EC within a region of the default mode network (DMN) by means of the SEM method and revealed the best model to represent this connectivity in people with Down syndrome.

Previous findings provide evidence that depression is related to abnormal patterns of fluctuating connectivity among brain regions accountable for the severity of this disorder and its characteristic pathological cognitive, behavioral and emotional manifestations. In particular, the DMN has been consistently reported to be impaired in patients with MDD and LLD, and its crucial role in the clinical neuroscience of these disorders has been clearly established (Guàrdia-Olmos et al., 2022; Wise et al., 2017). The DMN is a network of neural systems exhibiting increased activity in the absence of external demanding perceptual tasks (Raichle, 2015). It is implicated in self-referent processes, assigning value to stimuli and affecting laden behavioral withdrawal. Collectively considered, these processes lead depressed individuals to engage in maladaptive ruminative thoughts (Cooney et al., 2010; Hamilton et al., 2015; Jacob et al., 2020). Furthermore, increased DMN connectivity in MDD has been identified as a precursor of MDD (Li et al., 2017; Li et al., 2018; Pang et al., 2020; Posner et al., 2016). Nevertheless, some pieces of evidence point in a different direction: reduced connectivity within the DMN underlies depression (Li et al., 2019; Yan et al., 2019).

The literature regarding LLD is very limited compared to the number of reports on MDD. Here, we cite research that we believe illustrates the latest advances in disturbed DMN connectivity in LLD patients. On the one hand, Manning et al. (2019) claim that increased DMN activity is associated with an inability to regulate emotions in older patients with depression. On the other hand, Gandelman et al. (2019) characterized LLD by decreased DMN connectivity, and Wang et al. (2021) identified reduced posterior DMN connectivity as opposed to increased activation within the anterior DMN. However, these studies primarily examine functional connectivity, except for Li et al. (2017) and Li et al. (2019), and none of them employ SEM since the application of this approach to dynamic connectivity is currently starting to develop within the neuroimaging discipline.

To the best of our knowledge, no studies to date have explored dynamic effective connectivity within the DMN in persons with MDD using SEM. The few reported EC studies do not fully disclose the neural causal influences among the resting-state networks in LLD and, specifically, the putatively core disturbed network, the DMN. Considering the lack of data and the need for further advances in the dynamics of the complex brain, in the present study, we aimed to elucidate the dynamic effective connectivity in an LLD group compared to a control group. For this purpose, we employ SEM with resting-state fMRI in six regions of interest (ROIs) within the DMN aiming to (1) analyze the estimated dynamic connectivity models for each group by employing SEM and a lag 1 approach, (2) identify the complexity of the models for each group, and (3) compare the levels of complexity of the obtained models between both groups. This strategy allowed us to identify a neural model explaining EC dynamics in LLD and therefore apply this knowledge to develop early and more accurate diagnostic strategies for LLD. Moreover, in view of the abovementioned research, we hypothesize that (a) patients with LLD will show a more complex connectivity pattern within the DMN at rest considering the number of effects and its intensity than control individuals, and (b) this pattern will be reflected in the models that SEM will provide for each group, as this will constitute a possible biomarker for LLD. Finally, we justify the DMN selection based on two criteria. First, this network represents the main and most basic functioning regions of the DMN and should therefore be the most sensitive structure of all the subareas constituting the extensive DMN (Figueroa-Jiménez et al., 2021). Second, the computational difficulties arising from estimating a large number of possible structural models of the extensive DMN impose a series of restrictions regarding the limited number of ROIs and networks to consider.

2. Materials and methods

2.1. Participants

The initial sample was consisted of 59 persons, including 28 patients diagnosed with MDD and 31 healthy controls. Late-life MDD patients were consecutively recruited from the Department of Psychiatry at Bellvitge University Hospital (Barcelona, Spain). In all cases, major depression was the primary diagnosis, and the first depressive episode appeared after 40 years of age. The inclusion criteria for patients were (a) age between 60 and 75 years and (b) a formal diagnosis of primary late-life MDD. The exclusion criteria included (a) evidence of other past or current comorbid psychiatric diagnoses besides MDD, (b) substance use with the exception of nicotine, (c) intellectual disability, and (d) the presence of any inconvenience that prevented the person from undergoing a neuroimaging exam (e.g., prostheses or implants that are not compatible with fMRI equipment).

After fMRI acquisition, data from three subjects—one patient and two controls—were discarded due to excessive movement in one patient and one control (i.e., mean displacement values above the 1.5-mm threshold of framewise displacement for 3-mm isotropic voxels, as suggested by Soares et al. (2016) or Zhu et al. (2012)) and because of abnormally high scores for the depressive symptom scales in the other control participant. Thus, the final sample for this study was composed of a total of 56 participants, including 27 individuals with MDD (age: $M = 68.19$ and $SD = 4.048$; 74.1 % of women ($n_w = 20$)). The control group included 29 healthy persons age: $M = 67.9$ and $SD = 3.976$; 69.0 % women ($n_w = 20$). In MDD individuals, medication doses were maintained throughout the study.

2.2. Measures

After providing voluntary, written informed consent, participants

completed several cognitive and emotional assessments, including the Mini-Mental State Examination (MMSE) (Lobo et al., 1999), the vocabulary subtest of the Wechsler Adult Intelligence Scale, third edition (WAIS-III) (TEA Ediciones, 2001), the Geriatric Depression Scale (GDS) (Martínez et al., 2002), the Hamilton Depression Rating Scale (HDRS) (Conde and Franch, 1984) and the Spielberger State-Trait Anxiety Inventory (STAI) (Spielberger et al., 1982). MDD diagnoses were established according to DSM-IV-TR criteria, which do not substantially differ from the DSM-V criteria. See a further breakdown in the Supplementary materials.

2.3. Procedure

All participants were evaluated by the same clinical team designated for that purpose at Bellvitge University Hospital (Barcelona) affiliated with the University of Barcelona. The data registry was completed in three sessions: the first two for the questionnaires, scales and clinical interviews and the third for brain imaging. The protocol was approved by the Ethics Committee of Bellvitge University Hospital, and the research was performed in accordance with the ethical guidelines laid down in the 1964 Declaration of Helsinki and its later amendments (2013). All participants provided written informed consent for their participation.

Data storage followed the anonymity guidelines established by the European Data Management, and access was restricted to the accredited researchers. Rights to access and modification of the data were preserved for all participants in the study as stated in the informed consent that they signed.

2.4. MRI image acquisition and preprocessing

Each participant underwent an 8-minute resting-state fMRI scan in a 3 T Philips Ingenia scan (Philips Health care, Best, The Netherlands) using a 32-channel head coil. Scanning parameters are reported in the Supplementary materials.

2.5. Regions of interest

The regions of interest (ROIs) were defined by the Automatic Anatomical Labeling atlas (AAL) (Tzourio-Mazoyer et al., 2002). This atlas contains 90 cortical and subcortical areas, with 45 in each hemisphere. To acquire the full signal of a given ROI, the signal from within ROI voxels should be estimated through principal component analysis (PCA) at each time point across the entire time series. In this study, however, we focused on DMN ROIs according to the justification provided in the introduction. In particular, we evaluated the signal from six ROIs of the posterior DMN (pDMN) subnetwork, as detailed in Table 1 and whose spatial localization is represented in Fig. 1.

Table 1
Relationship of ROIs for the construction of the DMN according to the AAL90 atlas and their coordinates.

ROI	DMN				
	ROI AAL90	Region name	X	Y	Z
1	59	Parietal_Superior_Left	−23	−60	59
2	60	Parietal_Superior_Right	26	−59	62
3	61	Parietal_Inferior_Left	−43	−46	47
4	62	Parietal_Inferior_Right	46	−46	50
5	85	Temporal_Middle_Left	−56	−34	−2
6	86	Temporal_Middle_Right	57	−37	−1

Note. All the coordinates were extracted with a sphere radius of 10 mm (Tzourio-Mazoyer et al., 2002).

2.6. Statistical analysis

Sociodemographic and clinical data were analyzed with IBM SPSS (version 27.0.0). Between-group differences in quantitative variables were estimated with Student's *t*-test, while qualitative variables were assessed with the chi-square test. MANOVA was used to explore the interaction between a categorical independent variable and two continuous dependent variables. The level of significance was set to $p < .05$ for all tests.

Regarding the analysis of the imaging data, once the images were preprocessed, correlation matrices were obtained between the six ROIs mentioned in Table 1 for each subject evaluated. To avoid the aberrant effect of values in some especially high or low ROIs (outliers), the jackknife correlation was estimated. Other simulation possibilities exist when estimating statistical significance, but for small samples, this method is still recommended. This technique consists of calculating all the correlation coefficients between all the possible ROI pairs if one of the observations is excluded in each iteration. The average of all the correlations for each ROI pair attenuates the effects of the outliers. Each jackknife correlation coefficient is estimated using the following expression:

$$\theta_{(ROIi,ROIj)} = Jackknife\ Correlation\ Mean\ (ROIi, ROIj) = \frac{1}{n}\sum_{k=1}^{n} r_i$$

where r_i is Pearson's correlation between each pair of ROIs and n is the sample number in which the correlations in each pair have been estimated by extracting the record (volume) *i*. The *SE* of each average was also estimated from the expression:

$$SE = \sqrt{\frac{n-1}{n}\sum_{i=1}^{n}(r_i - \theta)^2}$$

This allows the confidence intervals' estimation for each correlation coefficient. Selecting between the correlation coefficient obtained with the whole sample or the coefficient obtained through jackknife estimation depends on the bias value obtained. The bias is defined by the following expression:

$$Bias = (n-1)^*(\theta - \widehat{r})$$

For each correlation between ROIs, the bias value was obtained, and when this value was close to 0, the average jackknife value was used. In cases where the bias was different from 0, the lower limit value of the confidence interval was used to avoid the probability of a type I error. To perform these analyses, the dist R library (3.6.2) was used. The different correlation matrices were used as input for the estimation of each SEM for each subject in both groups.

In essence, all structural models are adjusted by minimizing the matrix $(R - \Sigma)$. This expression involves reproduction (Σ) of the initial matrix of correlations (R) between ROIs from the combination of the estimation result of the parameters with statistical significance. In other words, the result shows the best possible model for each subject considering the incorporation of the recursive and nonrecursive effects between ROIs and incorporating the lag effects already described. A much broader description of SEMs applied to this context can be found in Guàrdia-Olmos et al. (2018), and since the SEM is exactly the same as DCM models under certain conditions, the difference in the current case, as already mentioned, is the incorporation of the dynamic effect.

3. Results

No statistically significant differences in age or sex were found between the patients and the healthy controls. Expectedly, patients had significantly higher scores on all the questionnaires administered. These demographic and clinical characteristics are presented in Table 2.

The results of the adjustment models for each participant according

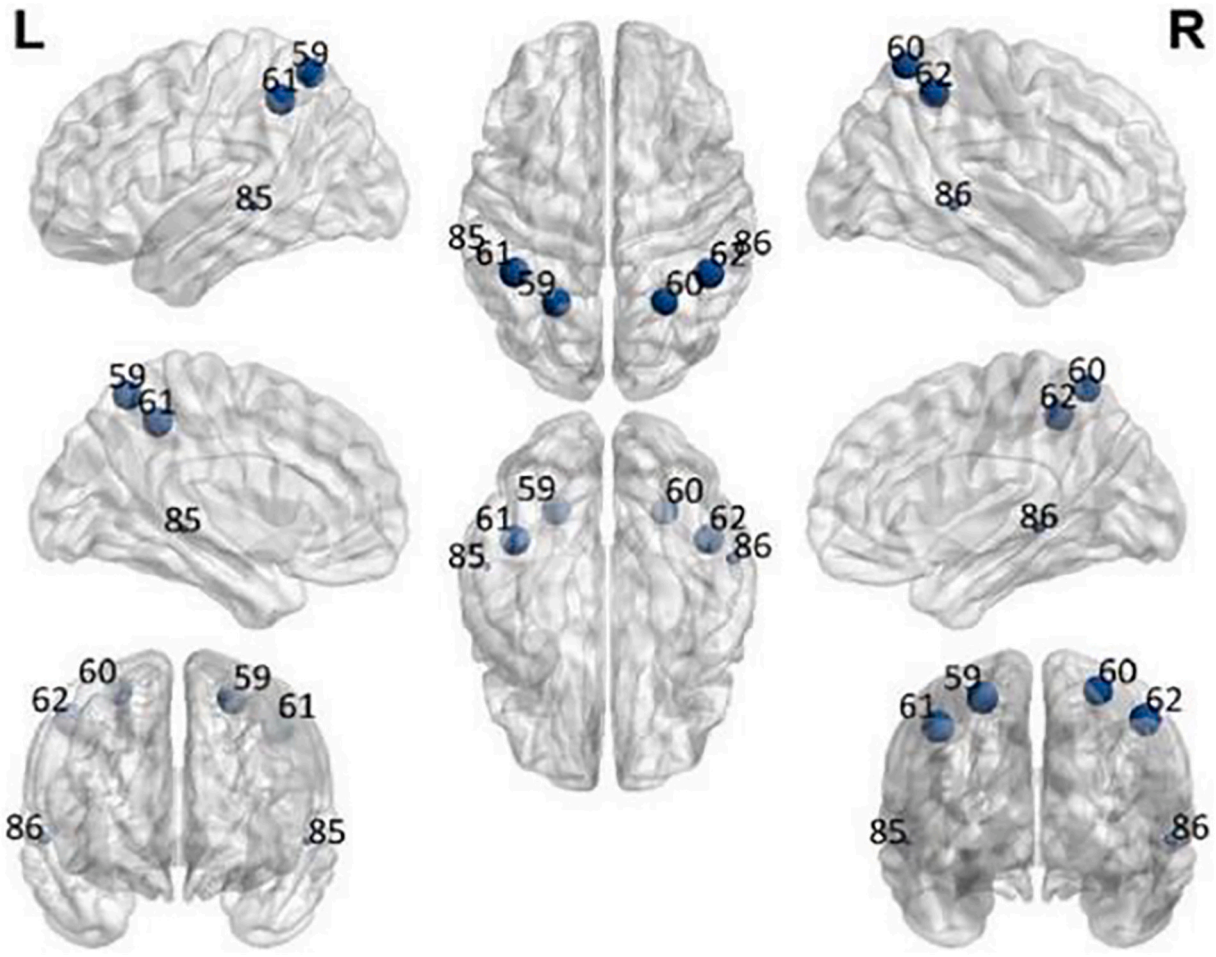

Fig. 1. Spatial localization of the six ROIs studied in the DMN.

Table 2
Demographic and clinical data.

	Healthy controls ($n = 29$)	Patients ($n = 27$)	Significance
Sex (M/F)	9/20	7/20	.672[a]
Age (mean, SD)	67.9 ± 3.976	68.19 ± 4.048	.789[b]
MMSE (mean, SD)	28.90 ± 1.398	26.74 ± 2.177	<.001[b,*]
WAIS-III (mean, SD)	45.17 ± 8.502	29.22 ± 7.382	<.001[b,*]
GDS (mean, SD)	0.90 ± 1.235	5.74 ± 4.503	<.001[b,*]
HDRS (mean, SD)	0.79 ± 1.177	11.56 ± 7.298	<.001[b,*]
STAI-S (mean, SD)	7.55 ± 5.748	24.93 ± 13.485	<.001[b,*]
STAI-T (mean, SD)	11.24 ± 6.345	29.67 ± 13.419	<.001[b,*]

MMSE, Mini Mental State Examination; WAIS-III, Weschler Adult Intelligence Scale; GDS, Geriatric Depression Scale; HDRS, Hamilton Depression Rating Scale; STAI-S, Spielberger's State Anxiety Inventory; STAI-T, Spielberger's Trait Anxiety Inventory.

[a] χ^2 test.

[b] Independent sample *t*-test.

[*] $p < .05$.

to the previously defined groups are displayed in Supplementary Table 1. This classification offers a modularity value of −0.0089, which confirms the nonexistence of communities other than the two proposed—a group of LLD persons and a group of healthy persons.

Table 3a describes the number of parameters with statistically significant effects for each of the six ROIs, including both synchronous and dynamic effects in the group of healthy persons. Likewise, Table 3b shows the same type of data in the group of persons with LLD. Fig. 2 visually summarizes these results with the total of statistically significant parameters.

Considering these results, we analyzed the concordance between the two groups regarding the different functions of the effects. We found that ROI 4 (parietal inferior right region) and ROI 6 (temporal middle right region) presented the highest variation between both groups in their synchronous and dynamic connections. ROI number 4 showed increased connections in the persons with MDD, but conversely, ROI number 6 exhibits greater connections in the control group. In addition, ROI 3 (parietal inferior left region) and ROI 5 (temporal middle left region) showed mild variation, being higher in the control group than the MDD group. The two remaining ROIs, ROI 1 (parietal superior left region) and ROI 2 (parietal superior right region), showed highly concordant effects with little difference between the groups.

Notably, these results suggest a heterogeneous distribution of the concordance and variation among effects between the groups. Moreover, throughout the six ROIs, we observe that the dynamic effects seem to be greater than the synchronous effects.

Fig. 3 illustrates the characteristic SEMs for each group, including all 29 participants in the control group (Fig. 3a) and all 27 subjects in the LLD group (Fig. 3b), at the same time.

Given these results, we also included the two best-fitting SEMs from each group as examples. These models are presented in Supplementary Fig. 1.

Our data show perfect accuracy in the correct classification of the 56 subjects in two different groups based on their effective connections over the pDMN: Group 1, referred to as the control group (29), and Group 2, referred to as the LLD group (27).

Table 3a
The number of statistically significant parameters in the group of control persons.

	Group number 1: Healthy controls											
	ROI1 lag	ROI2 lag	ROI3 lag	ROI4 lag	ROI5 lag	ROI6 lag	ROI1	ROI2	ROI3	ROI4	ROI5	ROI6
ROI1	29	29	6	1	4	7	0	29	7	2	6	7
ROI2	6	29	5	29	1	8	6	0	5	29	2	7
ROI3	29	4	29	3	4	5	29	4	0	4	4	3
ROI4	4	2	3	29	6	29	4	3	5	0	7	29
ROI5	8	5	29	5	29	29	8	6	29	6	0	29
ROI6	0	0	1	1	0	29	0	0	1	1	0	0

Table 3b
The number of statistically significant parameters in the group of people with LLD.

	Group number 2: Persons with LLD											
	ROI1 lag	ROI2 lag	ROI3 lag	ROI4 lag	ROI5 lag	ROI6 lag	ROI1	ROI2	ROI3	ROI4	ROI5	ROI6
ROI1	27	27	10	4	6	4	0	27	10	4	8	5
ROI2	6	27	4	27	4	3	6	0	5	27	5	3
ROI3	27	10	27	11	9	4	27	10	0	10	10	4
ROI4	0	0	1	27	5	0	0	1	1	0	5	1
ROI5	2	2	7	5	27	5	1	2	7	5	0	5
ROI6	8	8	4	27	8	27	9	9	4	27	8	0

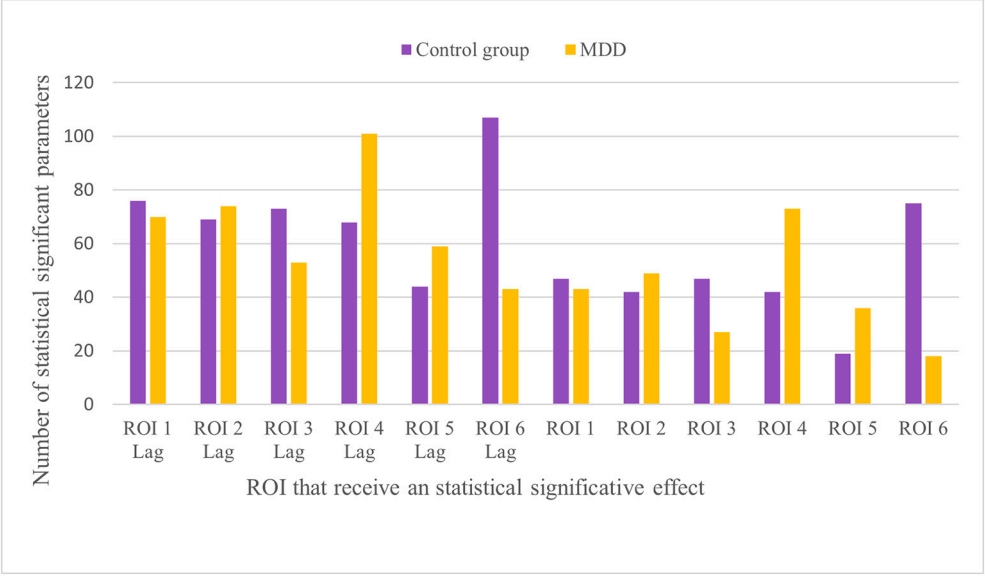

Fig. 2. The total number of statistically significant parameters for the two groups. Each column represents the number of effects that each ROI receives in a synchronous or dynamic (lag 1) situation.

Then, we explored the 66 possible connections between the six defined ROIs to compare the mean connectivity strengths. First, we examined the mean values of each effect considering all participants to elucidate which effects showed a significant directional connection. We found that among the 66 expected effects, 55 were significant. The remaining 10 are listed in Supplementary Table 2.

Next, we evaluated the differences in the significant effect values between the two groups by conducting independent samples *t*-tests comparing the mean connectivity strengths. Among the 55 significant effects between ROIs, only eight were found to be significantly different between the LLD group and the control group (see Supplementary Table 3 for details). The remaining differences were not significantly different from zero in either group. In addition, four of the significant effects corresponded to dynamic effects, while the other four corresponded to synchronous effects.

In the control group, 709 significant effects were obtained, while in the MDD group, 646 were detected, with a slightly greater number of effects in the control group. However, this difference in the number of estimated parameters was not statistically significant according to the comparison between both means [$t = 1.265$; $df = 54$; $p = .211$; *95 % CI difference* $= -0.522$–2.307]. The analysis of the values of the estimated parameters indicated the same lack of statistical significance [$t = -1.055$; $df = 54$; $p = .296$; *95 % CI difference* $= -0.011$–0.003].

With respect to the characteristics of the effects, we identified a total of 837 dynamic (lag 1) effects and 518 synchronous (lag 0) effects. This result clearly indicates a considerably higher number of dynamic effects compared to synchronous effects. In relation to the number of connections, we identified a statistically significant difference and a higher effect size between the two types of effects when comparing their means [$t = 54.346$; $df = 54$; $p < .001$; *95 % CI difference* $= 5.486$–5.906; $r = 0.90$]. In the case of the dynamic effects, the average was $M = 14.95$ ($SD = 1.407$), and for the synchronous effects, the average was $M = 9.25$ ($SD = 1.352$).

In addition, the possible interaction between the groups and the type

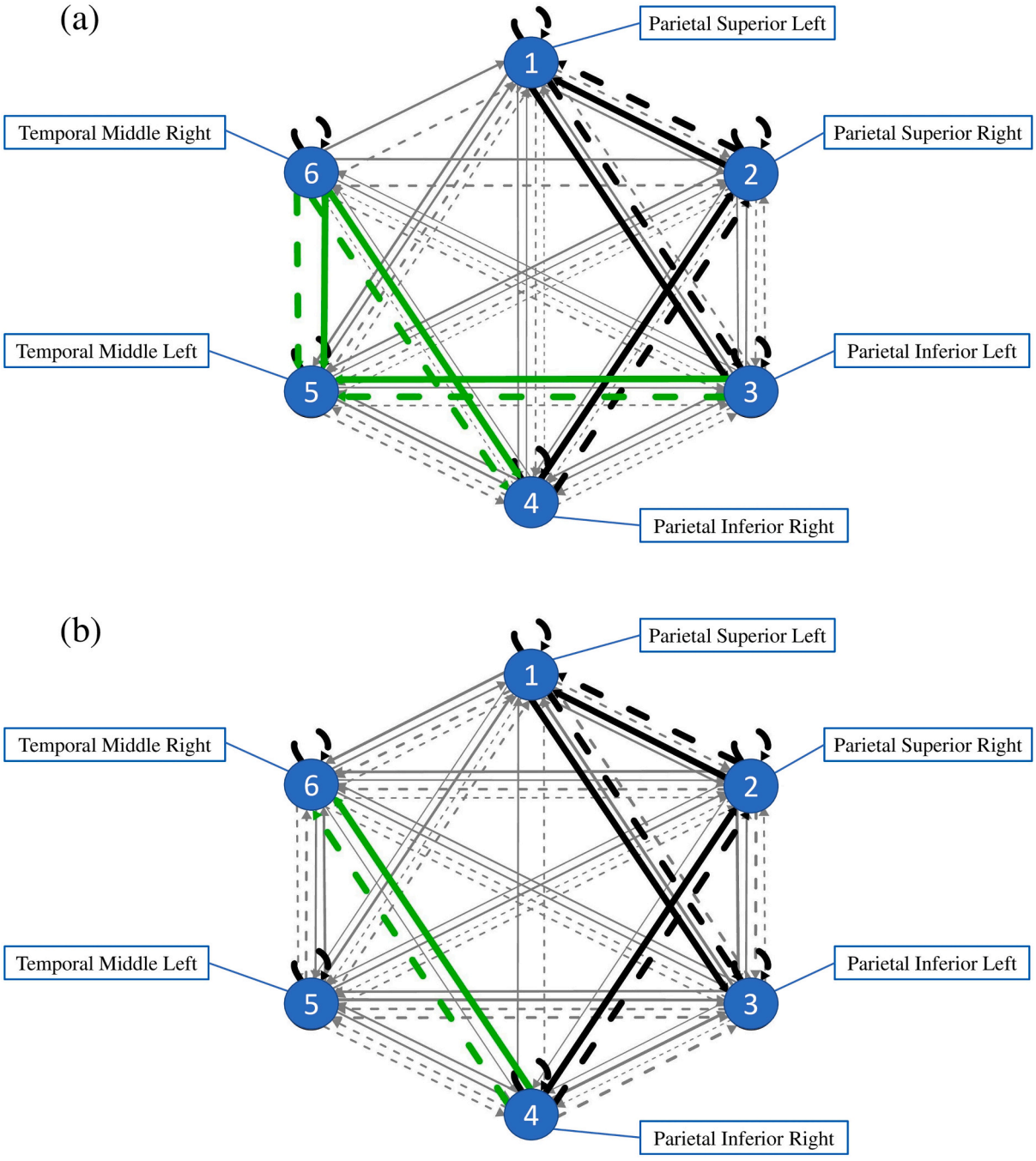

Fig. 3. Path diagram representations of each group: (a) the control group and (b) the MDD group. Black paths are at the group level, green paths are at the subgroup level, and gray paths are at the individual level; the thickness of the line represents the count.

of effects were tested through MANOVA, but no statistically significant effect was obtained [$F = 0.273$; $df = 2$ and 53; $p = .762$].

Therefore, the differences between the control group and the LLD group lie in the synchronous and dynamic effects regarding ROIs 4 and 6 as well as the overall dynamic effects that seem to be greater than the synchronous connections. Fig. 4 shows the most distinctive effects among the most frequent effects for each group, which allows us to visually identify the effects that are repeated the most and to differentiate each group along with the brain areas containing the connections.

4. Discussion

In this study, we recruited a group of patients with LLD and matched controls to investigate EC changes within the posterolateral DMN by comparing the results obtained in the adjustment of dynamic (lag 1) SEMs. Ultimately, the main goal was to identify the neural model best explaining the dynamic EC within the posterolateral DMN in persons with LLD.

The results obtained in this study lead us to assert that the dynamic EC in the pDMN is different between persons with depression and healthy controls. In fact, in classification analyses, we were able to identify the existence of two separate groups—a group of LLD persons and another group of control persons—defined by distinctive activation of the mentioned DMN subnetwork. Moreover, with our SEM, we achieved 100 % accuracy in classifying the subjects into either one of these two groups. These results are consistent with those of converging

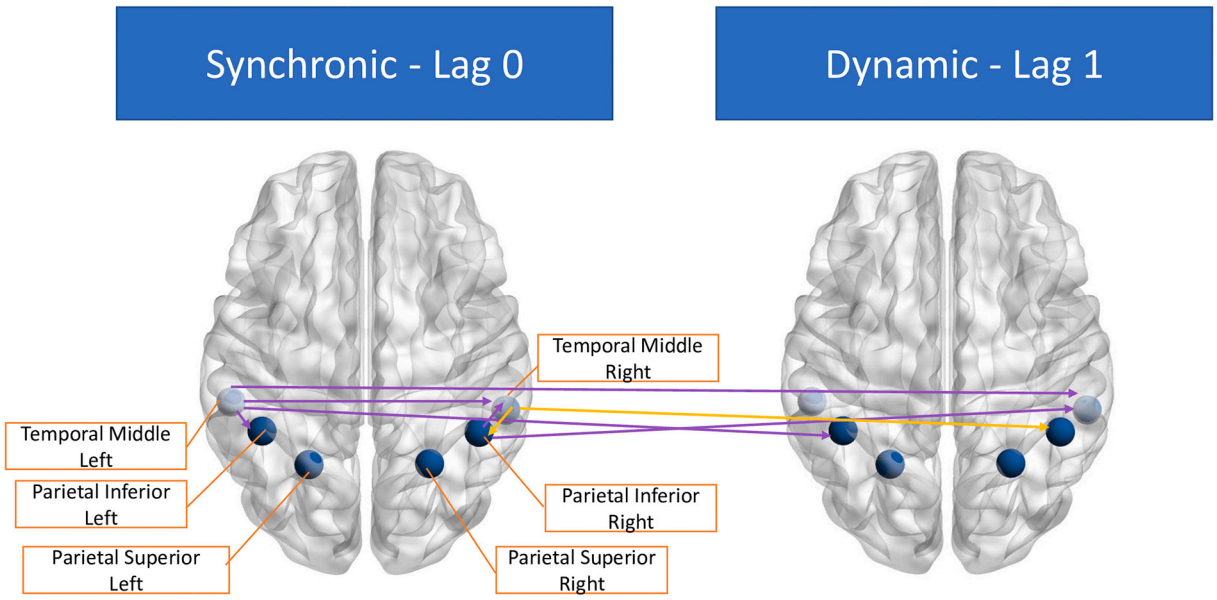

Fig. 4. Spatial representation of the structural equation model for each group considering the most distinctive frequent effects in both groups. Purple paths represent the control group, and yellow paths represent the MDD group. (For interpretation of the references to color in this figure legend, the reader is referred to the web version of this article.)

neuroimaging studies over recent years suggesting that posterior DMN connectivity alterations are nuclear in MDD (Li et al., 2019; Li et al., 2017; Li et al., 2016; Pang et al., 2020; Wise et al., 2017; Yan et al., 2019). Some of them have also obtained high percentages of classification between MDD and control persons; for instance, Khan et al. (2021) reached perfect accuracy.

The perfect classification found in this study is based on the existence of a network of effects that differentiate between the groups regarding ROI 4 (parietal inferior right region) and ROI 6 (temporal middle right region). These two ROIs had the largest number of effects in the LLD group and the control group. More precisely, our findings indicate that connections from ROI 6 (temporal middle right region) to ROI 4 (parietal inferior right region) and from ROI 3 (parietal inferior left region) to ROI 4, ROI 2lag (parietal superior right region) and ROI 5 (temporal middle left region) are the core set of effects that may lead to the pathological cognitive, behavioral and emotional manifestations of LLD.

Prior evidence has documented that the parietal inferior right region is primarily involved in several high cognitive functions, including interoception and the representation of subjective feeling states, inhibition of inappropriate responses, social and spatial cognition, reasoning and visuospatial attention (Luo et al., 2018; Wang et al., 2016). In MDD patients, this overactivation within the parietal inferior right region has been associated with impaired control of negative emotions (Wang et al., 2016). The enhanced connectivity in the parietal inferior right region might reflect a compensatory mechanism that MDD brains implement to achieve normal functioning. The characteristics of the disease imply impairment in the mentioned functions associated with the parietal inferior right region and, therefore, the brain is compelled to overactivate to achieve similar performance to that of healthy controls.

The revised literature does not suggest a robust link between the temporal middle right region and depression, which can be interpreted in two ways: first, our study method—SEM—has helped identify this prominent effect, or second, the effect may be abnormal. Thus, an additional study focusing on this specific ROI 6 is required.

Furthermore, the fact that the increased connectivity of the six ROIs studied appears to be distributed between the LLD group and the control group leads us to speculate that LLD brains overactivate those regions that, due to the nature of the disease, are more affected and thus develop a compensatory mechanism to maintain relatively normal cognitive performance. This idea of compensation has been postulated by other authors in their works, such as Zhang et al. (2018) and Zhu et al. (2012).

Compared to the number of synchronous effects, the number of dynamic (lagged) effects seemed to be greater throughout the six ROIs studied. The dynamic component was demonstrated to be the key in mapping the directed connectivity within the pDMN in LLD patients and constitutes the main difference between persons with LLD and healthy persons. This finding is in line with other evidence emphasizing the importance of dynamic connectivity to reveal significant aspects of brain connectivity in MDD (Bi et al., 2019; Kaiser et al., 2016). However, no studies have explored dynamic EC by means of SEM.

Some aspects of intrinsic network organization in the DMN might have been long overlooked. In this study, implementing the use of SEM and exploring dynamic connectivity helped us refine the results obtained by other colleagues and thus unveil the specific connections that characterize LLD. Here, we were able to elucidate the directed effects that discriminate between persons with LLD and healthy persons. Beyond the complexity based on the number of associations or its intensity, the shape that the specific connections adopt in their networks truly differentiates between people with depression and those considered to belong to the general population. In other words, what directed connections are established among the ROIs in the pDMN? In addition, the dynamics in these connectivity patterns are crucial elements that describe both groups.

The present study has some limitations. First, the sample size was limited to 56 participants. Therefore, the validity of the findings should be further tested in a larger sample. However, our sample is in line with the sample sizes of other related papers or even larger. Second, the LLD persons were taking various antidepressants and mood stabilizers, which is a variable that we did not control for and may have had some influence on our findings. This is a limitation in many studies on depression and is present in a large part of the revised literature. Third, we adopted a categorical perspective of depression—the presence or absence of MDD—but MDD is a heterogeneous disorder, and different subtypes of depression may produce unique patterns of abnormal dynamic connectivity. Finally, we also considered six ROIs of the DMN that constitute a small portion of the network even though they are considered the most representative ROIs.

However, this study had some strengths that must be highlighted.

The dynamic EC provides unique information about communication within the pDMN beyond that provided by static EC. Moreover, this paper shows for the first time that the structure of a dynamic connectivity network can perfectly discriminate between a group of people with LLD and a group of healthy controls.

The clinical relevance of this work is based on the fact that it provides a diagnostic tool complementary to those that already exist. This study, along with other compelling findings describing resting-state activation in MDD, establishes an emerging approach that might contribute to the accuracy of diagnosis. At present, connectivity studies are at an early stage, and therefore, we are in the early stages of drawing more specific conclusions. However, an important number of papers concerning dynamic brain connections have found differences between the population with cognitive and mental impairments and healthy persons. More research is needed to thoroughly disclose the nature of DMN connectivity and consistently identify an altered pattern of activation in persons with LLD that can undoubtedly constitute a biomarker for this disorder, which would allow early detection of LLD: even if patients do not show behavioral manifestations of their disorder, their brain connectivity may present certain properties compatible with characteristic LLD connectivity. This information could create a breakthrough in the early diagnosis of LLD and consequently facilitate the development of preventative treatments that might attenuate the progression of more severe symptomatology.

In summary, we provide new insight into the neurobiology of LLD that underlines the relevance of dynamic connectivity. The distinction between patients with LLD and controls is based on three aspects: the importance of ROIs 4 and 6, which seem to be the most distinctive among the subnetwork; the shape that the specific connections adopt in their networks, or in other words, the directed connections that are established among the ROIs in the pDMN for each group; and the number of dynamic effects that seem to be greater throughout the six ROIs studied. The network models that we developed according to the aims of the SEM describe a pattern of activation in the pDMN that constitutes a biomarker that can discriminate the levels of cognitive ability—those attributed to individuals with depression and healthy controls in this case.

Data availability statement

The data that support the findings of this study are available on request from the corresponding author. The data are not publicly available due to privacy or ethical restrictions.

Funding statement

This study was supported by the Agency for Management of University and Research Grants of the Catalan Government (2017SGR1247), the Carlos III Health Institute (Grants PIE14/00034, PI19/01040 and INT21/00055), the European Regional Development Fund (ERDF) “A way to build Europe”, and CIBERSAM.

Ethics approval statement

The protocol was approved by The Clinical Research Ethics Committee (CEIC) of Bellvitge University Hospital (reference PR156/15, 17th February 2016).

Patient consent statement

Informed consent was acquired from all participants.

CRediT authorship contribution statement

All authors contributed equally to the study conception and design. CSM, IC, MU, JMM, and VS. recruited the sample and collected the data, and JGO provided the resources for the study. RCG and JGO made the first conceptualizations of the paper, investigation, and methodology. Supervision of the paper was performed by CCM and MPC. The final review of the paper was performed by all authors.

Conflict of interest

The authors declare that they have no conflicts of interest.

Acknowledgments

The authors would like to thank the study participants and the staff from Bellvitge University Hospital and Institut de Diàgnostic per la Imatge (IDI) who contributed to recruiting the study sample. We also thank CERCA Programme/Generalitat de Catalunya for institutional support and Ministerio de Ciencia, Innovación y Universidades, Agencia Estatal de Investigación. Grant Number: PGC2018-095829-B-100.

Appendix A. Supplementary data

Supplementary data to this article can be found online at https://doi.org/10.1016/j.jad.2022.09.010.

References

American Psychiatric Association, 2013. Diagnostic and Statistical Manual of Mental Disorders, 5th ed. American Psychiatric Publishing.

Beltz, A.M., Gates, K.M., 2017. Network mapping with GIMME. Multivar. Behav. Res. 52 (6), 789–804. https://doi.org/10.1080/00273171.2017.1373014.

Bi, K., Luo, G., Tian, S., Zhang, S., Liu, X., Wang, Q., Lu, Q., Yao, Z., 2019. An enriched granger causal model allowing variable static anatomical constraints. NeuroImage: Clin. 21 https://doi.org/10.1016/j.nicl.2018.11.002.

Conde, V., Franch, J.I., 1984. Escalas de evaluación comportamental para la cuantificación de la sintomatología psicopatológica en los trastornos angustiosos y depresivos. Departamento de psicología médica y de psiquiatría del Hospital Clínico de la Facultad de Medicina.

Cooney, R.E., Joormann, J.E.F., Dennis, E.L., Gotlib, I.H., 2010. Neural correlates of rumination in depression. Cogn. Affect. Behav. Neurosci. 10 (4), 470–478. https://doi.org/10.3758/CABN.10.4.470.

Figueroa-Jiménez, M.D., Cañete-Massé, C., Carbó-Carrete, M., Zarabozo-Hurtado, D., Guàrdia-Olmos, J., 2021. Structural equation models to estimate dynamic effective connectivity networks in resting fMRI. A comparison between individuals with down syndrome and controls. Behav. Brain Res. 405 https://doi.org/10.1016/j.bbr.2021.113188.

Friston, K.J., 2011. Functional and effective connectivity: a review. Brain Connect. 1 (1), 13–36. https://doi.org/10.1089/brain.2011.0008.

Friston, K.J., Kahan, J., Biswal, B., Razi, A., 2014. A DCM for resting state fMRI. NeuroImage 94, 396–407. https://doi.org/10.1016/j.neuroimage.2013.12.009.

Gandelman, J.A., Albert, K., Boyd, B.D., Park, J.W., Riddle, M., Woodward, N.D., Kang, H., Landman, B.A., Taylor, W.D., 2019. Intrinsic functional network connectivity is associated with clinical symptoms and cognition in late life depression. Biol. Psychiatry: Cogn. Neurosci. Neuroimaging 4 (2), 160–170. https://doi.org/10.1016/j.bpsc.2018.09.003.

Gates, K.M., Molenaar, P.C.M., Hillary, F.G., Slobounov, S., 2011. Extended unified SEM approach for modeling event-related fMRI data. NeuroImage 54 (2), 1151–1158. https://doi.org/10.1016/j.neuroimage.2010.08.051.

Guàrdia-Olmos, J., Peró-Cebollero, M., Gudayol-Ferré, E., 2018. Meta-analysis of the structural equation models' parameters for the estimation of brain connectivity with fMRI. Front. Behav. Neurosci. 12, 19. https://doi.org/10.3389/fnbeh.2018.00019.

Guàrdia-Olmos, J., Soriano-Mas, C., Tormo-Rodríguez, L., Cañete-Massé, C., del Cerro, I., Urretavizcaya, M., Menchón, J.M., Soria, V., Peró-Cebollero, M., 2022. Abnormalities in the default mode network in late-life depression: a study of resting-state fMRI. Int. J. Clin. Health Psychol. 22 (3) https://doi.org/10.1016/j.ijchp.2022.100317.

Gunning, F.M., Oberlin, L.E., Schier, M., Victoria, L.W., 2021. Brain-based mechanisms of late-life depression: implications for novel interventions. Semin. Cell Dev. Biol. 116, 169–179. https://doi.org/10.1016/j.semcdb.2021.05.002.

Hamilton, J.P., Farmer, M., Fogelman, P., Gotlib, I.H., 2015. Depressive rumination, the default-mode network, and the dark matter of clinical neuroscience. Biol. Psychiatry 78 (4), 224–230. https://doi.org/10.1016/j.biopsych.2015.02.020.

Inman, C.S., James, G.A., Hamann, S., Rajendra, J.K., Pagnoni, G., Butler, A.J., 2012. Altered resting-state effective connectivity of fronto-parietal motor control systems on the primary motor network following stroke. NeuroImage 59 (1), 227–237. https://doi.org/10.1016/j.neuroimage.2011.07.083.

Jacob, Y., Morris, L.S., Huang, K.H., Schneider, M., Rutter, S., Verma, G., Murrough, J. W., Balchandani, P., 2020. Neural correlates or rumination in major depressive disorder : a brain network analysis. NeuroImage : Clin. 25 https://doi.org/10.1016/j.nicl.2019.102142.

Joormann, J., Stanton, C.H., 2016. Examining emotion regulation in depression: a review and future directions. Behav. Res. Ther. 86, 35–49. https://doi.org/10.1016/j.brat.2016.07.007.

Kaiser, R.H., Whitfield Gabrieli, S., Dillon, D.G., Goer, F., Beltzer, M., Minkel, J., Smoski, M., Dichter, G., Pizzagalli, D.A., 2016. Dynamic resting-state functional connectivity in major depression. Neuropsychopharmacology 41 (7), 1822–1830. https://doi.org/10.1038/npp.2015.352.

Khan, D., Yahya, N., Kamel, N., Faye, I., 2021. Automated diagnosis of major depressive disorder using brain effective connectivity and 3D convolutional neural network. IEEE Access 9, 8835–8846. https://doi.org/10.1109/ACCESS.2021.3049427.

Li, B., Friston, K., Mody, M., Wang, H.N., Lu, H.B., Hu, D.W., 2018. A brain network model for depression: from symptom understanding to disease intervention. CNS Neurosci. Ther. 24 (11), 1004–1019. https://doi.org/10.1111/cns.12998.

Li, L., Li, B., Bai, Y., Liu, W., Wang, H., Leung, H.C., Tian, P., Zhang, L., Guo, F., Cui, L.B., Yin, H., Lu, H., Tan, Q., 2017. Abnormal resting state effective connectivity within the default mode network in major depression disorder: a spectral dynamic causal modeling study. Brain Behav. 7 (7) https://doi.org/10.1002/brb3.732.

Li, L., Li, B., Bai, Y., Wang, H., Zhang, L., Cui, L., Lu, H., 2016. Altered effective connectivity within default mode network in major depression disorder. J. Med. Imaging 9789. https://doi.org/10.1117/12.2218363.

Li, G., Liu, Y., Zheng, Y., Li, D., Liang, X., Chen, Y., Cui, Y., Yap, P.T., Qiu, S., Zhang, H., Shen, D., 2019. Large scale dynamic causal modeling of major depressive disorder based on resting-state functional magnetic resonance imaging. Hum. Brain Mapp. 41 (4), 865–881. https://doi.org/10.1002/hbm.24845.

Lobo, A., Saz, P., Marcos, G., Día, J.L., de la Cámara, C., Ventura, T., Morales Asín, F., Pascual, L.F., Montañés, J.A., Aznar, S., 1999. Revalidación y normalización del mini-examen cognoscitivo (primera versión en castellano del mini-mental status Examination) en la población general geriátrica. Med. Clin. 112, 767–774.

Luo, L., Wu, K., Lu, Y., Gao, S., Kong, X., Lu, F., Wu, F., Wu, H., Wang, J., 2018. Increased functional connectivity between medulla and inferior parietal cortex in medication-free major depressive disorder. Front. Neurosci. 12 (926) https://doi.org/10.3389/fnins.2018.00926.

Manning, K., Wang, L., Steffens, D., 2019. Recent advances in the use of imaging in psychiatry: functional magnetic resonance imaging of large-scale brain networks in late-life depression. F1000 Research 8. https://doi.org/10.12688/f1000research.17399.1.

Martínez, J., Onís, M.C., Dueñas, R., Albert, C., Aguado, C., Luque, R., 2002. Versión española del cuestionario de yesavage abreviado (GDS) Para el despistaje de depresión en mayores de 65 años: adaptación y validación. Rev. Med. Fam. Comunitaria 12 (10), 620–630. https://doi.org/10.4321/S1131-57682002001000003.

Pang, Y., Zhang, H., Cui, Q., Yang, Q., Lu, F., Chen, H., He, Z., Wang, Y., Wang, J., Chen, H., 2020. Aust. N. Z. J. Psychiatry 54 (8), 832–842. https://doi.org/10.1177/0004867420924089.

Posner, J., Cha, J., Wang, Z., Talati, A., Warner, V., Gerber, A., Peterson, B.S., Weissman, M., 2016. Increased default mode network connectivity in individuals at high risk for depression. Neuropsychopharmacology 41 (7), 1759–1767. https://doi.org/10.1038/npp.2015.342.

Raichle, M.E., 2015. The brain's default mode network. Annu. Rev. Neurosci. 38, 433–447. https://doi.org/10.1146/annurev-neuro-071013-014030.

Razi, A., Friston, K.J., 2016. The connected brain: causality, models and instrinsic dynamic. IEEE Signal Process. Mag. 33 (3), 14–35. https://doi.org/10.1109/MSP.2015.2482121.

Razi, A., Kahan, J., Rees, G., Friston, K.J., 2015. Construct validation of a DCM for resting state fMRI. NeuroImage 106, 1–14. https://doi.org/10.1016/j.neuroimage.2014.11.027.

Razi, A., Seghier, M.L., Zhou, Y., McColgan, P., Zeidman, P., Park, H.J., Sporns, O., Rees, G., Friston, K.J., 2017. Large-scale DCMs for resting-state fMRI. Neuroscience 1 (3), 222–241. https://doi.org/10.1016/j.neuroimage.2014.11.027.

Sartorius, N., 2001. The economic and social burden of depression. J. Clin. Psychiatry 62 (Supplement 15), 8–11.

Soares, J.M., Magalhães, R., Moreira, P.S., Sousa, A., Ganz, E., Sampaio, A., Alves, V., Marques, P., Sousa, N., 2016. A Hitchhiker's guide to functional magnetic resonance imaging. Front. Neurosci. 10 (515) https://doi.org/10.3389/fnins.2016.00515.

Spielberger, C.D., Gorsuch, R.L., Lushene, R., 1982. Manual del Cuestionario de Ansiedad Estado/Rasgo (STAI). TEA Ediciones.

TEA Ediciones, 2001. WAIS-III. Escala de inteligencia Weschler para adultos-III. TEA Ediciones.

Tzourio-Mazoyer, N., Landeau, B., Papathanassiou, D., Crivello, F., Etard, O., Delcroix, N., Mazoyer, B., Joliot, M., 2002. Automated anatomical labeling of activations in SPM using a macroscopic anatomical parcellation of the MNI MRI single-subject brain. NeuroImage 15 (1), 273–289. https://doi.org/10.1006/nimg.2001.0978.

Wang, S.M., Kim, N.Y., Um, Y.H., Kang, D.W., Na, H.R., Lee, C.U., Lim, H.K., 2021. Default mode network dissociation linking cerebral beta amyloid retention and depression in cognitively normal older adults. Neuropsychopharmachology 46, 2180–2187. https://doi.org/10.1038/s41386-021-01072-9.

Wang, J., Zhang, J., Rong, M., Wei, X., Zheng, D., Fox, P.T., Eickhoff, S.B., Zang, T., 2016. Functional topography of the right inferior parietal lobule structured by anatomical connectivity profiles. Hum. Brain Mapp. 37, 4316–4332. https://doi.org/10.1002/hbm.23311.

Wen, J., Fu, C.H.Y., Tosun, D., Veturi, Y., Yang, Z., Abdulkadir, A., Mamourian, E., Srinivasan, D., Skampardoni, I., Singh, A., Nawani, H., Bao, J., Erus, G., Shou, H., Habes, M., Doshi, J., Varol, E., Mackin, R.S., Sotiras, A., Davatzikos, C., 2022. Characterizing heterogeneity in neuroimaging, cognition, clinical symptoms, and genetics among patients with late-life depression. JAMA Psychiatry 79 (5), 464–474. https://doi.org/10.1001/jamapsychiatry.2022.0020.

Wise, T., Marwood, L., Perkins, A.M., Harane-Vives, A., Joules, R., Lythgoe, D.L., Luh, W. M., Williams, S.C.R., Young, A.H., Cleare, A.J., Arnone, D., 2017. Instability of default mode network connectivity in major depression: a two sample confirmation study. Transl. Psychiatry 7 (4). https://doi.org/10.1038/tp.2017.40.

Yan, C.G., Chen, X., Li, L., Castellanos, F.X., Bai, T.J., Bo, Q.J., Cao, J., Chen, G.M., Chen, N.X., Chen, W., Cheng, C., Cheng, Y.Q., Cui, X.L., Duan, J., Fang, Y.R., Gong, Q.Y., Guo, W.B., Hou, Z.H., Hu, L., Zang, Y.F., 2019. Reduced default mode network functional connectivity in patients with recurrent major depression disorder. PNAS 116 (18), 9078–9083. https://doi.org/10.1073/pnas.1900390116.

Zarghami, T.S., Friston, K.J., 2020. Dynamic effective connectivity. NeuroImage 207. https://doi.org/10.1016/j.neuroimage.2019.116453.

Zhang, S., Tian, S., Chattun, M.R., Tang, H., Yan, R., Bi, K., Yao, Z., Lu, Q., 2018. A supplementary functional connectivity microstate attached to the default mode network in depression revealed by resting-state magnetoencephalography. Prog. Neuro-Psychopharmacol. Biol. Psychiatry 83, 76–85. https://doi.org/10.1016/j.pnpbp.2018.01.006.

Zhang, X., Yang, J., Wang, R., Li, P., 2020. A neuroimaging study of semantic representation in first and second languages. Lang. Cogn. Neurosci. 35 (10) https://doi.org/10.1080/23273798.2020.1738509.

Zhu, X., Wang, X., Xiao, J., Liao, J., Zhong, M., Wang, W., Yao, S., 2012. Evidence of a dissociation pattern in resting-state default mode network connectivity in first-episode, treatment-naive major depression patients. Biol. Psychiatry 71 (7), 611–617. https://doi.org/10.1016/j.biopsych.2011.10.035.